University of Reading

On the role of specific interactions in the diffusion of nanoparticles in aqueous polymer solutions

Article

Published Version

Creative Commons: Attribution 3.0 (CC-BY)

Mun, E. A., Hannell, C., Rogers, S. E., Hole, P., Williams, A. C. ORCID: https://orcid.org/0000-0003-3654-7916 and Khutoryanskiy, V. V. ORCID: https://orcid.org/0000-0002-7221-2630 (2014) On the role of specific interactions in the diffusion of nanoparticles in aqueous polymer solutions. Langmuir, 30 (1). pp. 308-317. ISSN 0743-7463 doi: https://doi.org/10.1021/la4029035 Available at https://centaur.reading.ac.uk/35681/

It is advisable to refer to the publisher's version if you intend to cite from the work. See Guidance on citing.

Published version at: http://pubs.acs.org/doi/abs/10.1021/la4029035?prevSearch=Khutoryanskiy&searchHistoryKey=

To link to this article DOI: http://dx.doi.org/10.1021/la4029035

Publisher: American Chemical Society

All outputs in CentAUR are protected by Intellectual Property Rights law, including copyright law. Copyright and IPR is retained by the creators or other copyright holders. Terms and conditions for use of this material are defined in the End User Agreement.

www.reading.ac.uk/centaur

University of Reading

CentAUR

Central Archive at the University of Reading

Reading's research outputs online

Langmuir

Article

pubs.acs.org/Langmuir

Terms of Use CC-BY

On the Role of Specific Interactions in the Diffusion of Nanoparticles in Aqueous Polymer Solutions

Ellina A. Mun,[†] Claire Hannell,[‡] Sarah E. Rogers,[§] Patrick Hole,[‡] Adrian C. Williams,[†] and Vitaliy V. Khutoryanskiy*,[†]

[†]Reading School of Pharmacy, University of Reading, Whiteknights, P.O. Box 224, Reading, Berkshire RG6 6AD, U.K.

[‡]NanoSight Ltd, Minton Park, London Road, Amesbury SP4 7RT, U.K.

[§]ISIS Spallation Neutron Source, Science and Technology Facilities Council, Rutherford Appleton Laboratory, Harwell Science and Innovation Campus, Didcot, OX11 0QX U.K.

Supporting Information

ABSTRACT: Understanding nanoparticle diffusion within non-Newtonian biological and synthetic fluids is essential in designing novel formulations (e.g., nanomedicines for drug delivery, shampoos, lotions, coatings, paints, etc.), but is presently poorly defined. This study reports the diffusion of thiolated and PEGylated silica nanoparticles, characterized by small-angle neutron scattering, in solutions of various water-soluble polymers such as poly(acrylic acid) (PAA), poly(*N*-vinylpyrrolidone) (PVP), poly(ethylene oxide) (PEO), and hydroxyethylcellulose (HEC) probed using NanoSight nanoparticle tracking analysis. Results show that the diffusivity of nanoparticles is affected by their dimensions, medium viscosity, and, in particular, the specific interactions between nanoparticles and the macromolecules in solution; strong attractive interactions such as hydrogen bonding hamper diffusion. The water-soluble polymers retarded the diffusion of thiolated particles in the order PEO > PVP > PAA > HEC whereas for PEGylated silica particles retardation followed the order PAA > PVP = HEC > PEO. In the absence of specific interactions with the medium, PEGylated nanoparticles exhibit enhanced mobility compared to their thiolated counterparts despite some increase in their dimensions.

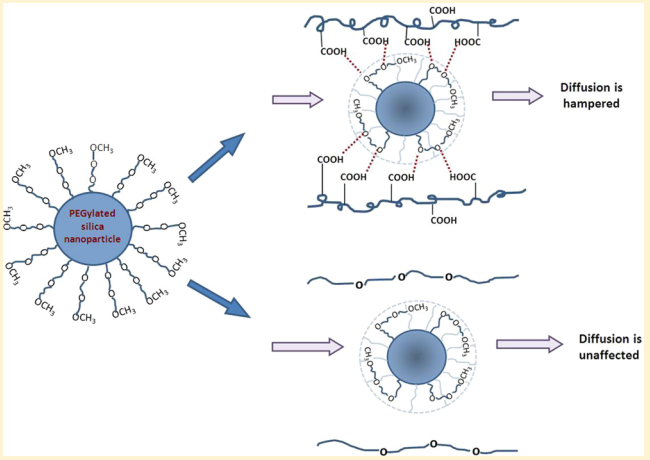

The diffusion of small particles suspended in liquids has received a lot of attention since 1905, when Albert Einstein published his pioneering work presenting a theoretical analysis of this phenomenon.[1] He demonstrated that the diffusion coefficient of small spherical particles is related to the absolute temperature and is inversely proportional to the particle size and to the viscosity of the liquid medium. The Stokes−Einstein equation is now widely used to describe the diffusion of small spherical particles in liquid media

$$D = \frac{kT}{3\pi\eta d}$$

where D is the diffusion coefficient, k is the Boltzmann constant, T is the absolute temperature, η is the dynamic viscosity, and d is the particle diameter.

The diffusion of nano- and microparticles in non-Newtonian fluids is a complex transport phenomenon that cannot simply be described by the Stokes−Einstein equation[2] and is still not fully understood. In the paint and coating industry, understanding diffusion is important to describing how multi-particulate systems can be efficiently mixed and how quickly particles will sediment and form a uniform coating layer upon system drying. In cosmetics, the diffusion of nanomaterials in complex formulations such as shampoos and lotions often affects their deposition onto hair and skin surfaces and determines the application efficiency. There are also a number of biological processes that rely on diffusion. For example, the penetration of the body by viruses and bacteria is often prevented by protective viscoelastic biological gels on mucosal surfaces. In the airway, this mucus gel traps microorganisms that are then eliminated through mucociliary clearance.[3]

Understanding the factors affecting the diffusion of nanoparticles in complex fluids is particularly important for drug delivery. A number of therapeutic areas can benefit greatly from nanomaterials with enhanced abilities to diffuse through viscous biological fluids and gels, for example, in delivering drug and

Received: July 29, 2013
Revised: November 12, 2013
Published: December 19, 2013

 © 2013 American Chemical Society dx.doi.org/10.1021/la4029035 | *Langmuir* 2014, 30, 308−317

gene nanocarriers to manage or treat cystic fibrosis. This life-threatening inherited condition causes the body to produce excessive quantities of thick mucus, which blocks the lungs and also affects the digestive tract and other organs and functions.[4] Similarly, a number of ocular degenerative conditions could potentially be efficiently treated via intraocular injections, where the facilitated diffusion of nanocarriers through the vitreous gel is essential for successful therapy[5] and poor diffusion through viscous vaginal fluids limits some therapies for sexually transmitted infections.[6]

Recently, Hanes and co-workers have reported a series of studies[7,8] demonstrating that 220 nm negatively charged polystyrene nanoparticles, which usually diffuse poorly through mucus, can be coated with short-chain poly(ethylene glycol) (PEG) to enhance their penetration of gels dramatically. The densely PEGylated nanoparticles possess hydrophilic and near neutrally charged surfaces that minimize mucoadhesion by reducing hydrophobic or electrostatic interactions, which mimics the ability of viruses to diffuse efficiently through mucus. Additionally, depending on the molecular weight (M_w) of the PEG, the nanoparticles can be made mucus-penetrating (when M_w is 2000 Da) or mucoadhesive (when M_w is 10 000 Da).

In this work, we have developed a series of fluorescently labeled thiolated and PEGylated silica nanoparticles to study their diffusion behavior in solutions of different water-soluble polymers. Particles were characterized using small-angle neutron scattering, and for the first time, we have utilized NanoSight Nanoparticle Tracking Analysis (NTA) to visualize nanoparticle diffusion in various media. This technique provides the important ability to measure the diffusion coefficients of fluorescent nano-objects without interference from other components (such as nonfluorescent macromolecules) present in the medium. Through the rational selection of different water-soluble polymers, we demonstrate that specific interactions between the components of this complex mixture can dramatically affect the diffusivity of nanoparticles.

MATERIALS AND METHODS

Materials. (3-Mercaptopropyl)trimethoxysilane (MPTS, 95%), methoxypoly(ethylene glycol) maleimide with average molecular weights of 750 and 5000 Da (PEG 750 and PEG 5000, respectively), 2-hydroxyethyl cellulose (HEC, MW 90 000 Da), poly(acrylic acid) (PAA, MW 450 000 Da), poly(ethylene oxide) (PEO, MW 1 000 000 Da), poly(vinylpyrrolidone) (PVP, MW 360 000 Da), 5,5′-dithiobis(2-nitrobenzoic acid) (DTNB), and L-cysteine hydrochloride were purchased from Sigma-Aldrich, Inc. (U.K.) and used as received. Alexa Fluor 546 C_5 maleimide, used for the synthesis of fluorescently labeled nanoparticles, was purchased from Invitrogen, Life Technologies (USA). Dimethyl sulfoxide (DMSO) and sodium hydroxide (NaOH) were purchased from Fisher Scientific Ltd. (U.K.) and were laboratory-grade reagents.

Synthesis of Thiolated and PEGylated Nanoparticles. Organosilica nanoparticles were synthesized according to the slightly modified protocol introduced by Irmukhametova et al.[9,10] Briefly, 0.75 mL of MPTS was mixed with 20 mL of DMSO and 0.5 mL of a 0.5 mol/L NaOH aqueous solution. The reaction was conducted with air bubbling and allowed to proceed for 24 h under constant stirring at room temperature. Synthesized nanoparticles were purified by dialysis against deionized water (5 L, eight changes of water) using dialysis tubing with a 12 000−14 000 Da molecular weight cut off (Medicell International Ltd., U.K.). PEGylation of nanoparticles was achieved by mixing 5 mL of thiolated nanoparticles with 100 mg of methoxypoly(ethylene glycol) maleimide of two molecular weights (750 and 5000 Da). The reaction mixture was stirred for 16 h at room temperature. PEGylated nanoparticles were purified by dialysis as above.

Synthesis of Fluorescently Labeled Nanoparticles. Fluorescently labeled nanoparticles were synthesized by mixing 1 mg of Alexa Fluor 546 C_5 maleimide with 17 mL of an aqueous dispersion of nanoparticles (7.4 mg/mL). This mixture corresponds to 1 μmol of the fluorescent dye per 50 μmol of SH groups in the nanoparticles. The reaction was allowed to proceed for 5.5 h under constant stirring at room temperature and protection from light with aluminum foil. The fluorescently labeled nanoparticles were purified by dialysis in the dark according to the protocol described above. Fluorescently labeled PEGylated nanoparticles were synthesized by mixing 5 mL of fluorescently labeled nanoparticles with 100 mg of methoxypoly(ethylene glycol) maleimide of two molecular weights (750 and 5000 Da). The reaction mixture was stirred for 16 h at room temperature, protected from light. PEGylated nanoparticles were purified by dialysis in the dark as above.

Dynamic Light Scattering. The size of nanoparticles was determined by dynamic light scattering using a Nano-S Zetasizer (Malvern Instruments, U.K.) at 25 °C. Each sample was analyzed three times, and the data are presented as the mean ± standard deviation.

Transmission Electron Microscopy (TEM). TEM images of thiolated and PEGylated nanoparticles were acquired using a Philips CM20 Analytical TEM operating at acceleration voltages of 80 and 200 kV. A drop of a nanoparticle dispersion was placed on the carbon-coated Cu grid for 1 min and dried with filter paper before images were collected.

Small-Angle Neutron Scattering (SANS). Aqueous dispersions of nanoparticles were dialized against deuterium oxide for 48 h prior to the experiment. SANS experiments were performed on the time-of-flight LOQ diffractometer at the ISIS neutron facility, U.K. The incident wavelength range of 2.2−10 Å gave rise to a Q range of 0.009−0.249 Å^{-1} where Q is defined as

$$Q = \frac{4\pi \sin\frac{\theta}{2}}{\lambda}$$

θ is the scattering angle, and λ is the neutron incident wavelength. Each sample and background (D_2O) were placed in 2-mm-path-length quartz cuvettes and were measured for 40 min in order to gather data of high statistical precision. Raw scattering data sets were corrected for detector efficiencies, sample transmission, and background scattering and converted to scattering cross-section data ($\partial\Sigma/\partial\Omega$ vs Q) using instrument-specific software.[11,12] Absolute intensities for $I(Q)$ (cm^{-1}) were determined within 5% by measuring the scattering from a partially deuterated polymer standard.[13] The SasView analysis program (http://www.sasview.org) was used for data modeling. Spherical form factor $P(Q)$ was employed for all data analysis with the addition of core−shell scattering length densities and shell thickness parameters for the two coated nanoparticles. The form factor for spheres is given as

$$P(Q) = \frac{\text{scale}}{V}\left[\frac{3V(\Delta\rho)[\sin(Qr) - Qr\cos(Qr)}{(Qr)^3}\right]^2 + bkg$$

where scale is the scale factor (in this case, the volume fraction), V is the volume of the scatterer, r is the radius of the sphere, bkg is the background level, and $\Delta\rho$ is the scattering length density difference between the scatterer and the solvent. This form factor is modified for the core−shell model as follows

$$P(Q) = \frac{\text{scale}}{V_s}\left[\frac{3V_c(\rho_c - \rho_s)[\sin(Qr_c) - Qr_c\cos(Qr_c)}{(Qr_c)^3} + \frac{3V_s(\rho_s - \rho_{solv})[\sin(Qr_s) - Qr_c\cos(Qr_s)}{(Qr_s)^3}\right]^2 + bkg$$

where subscripts c, s, and solv represent the core, shell, and solvent, respectively.

dx.doi.org/10.1021/la4029035 | Langmuir 2014, 30, 308−317

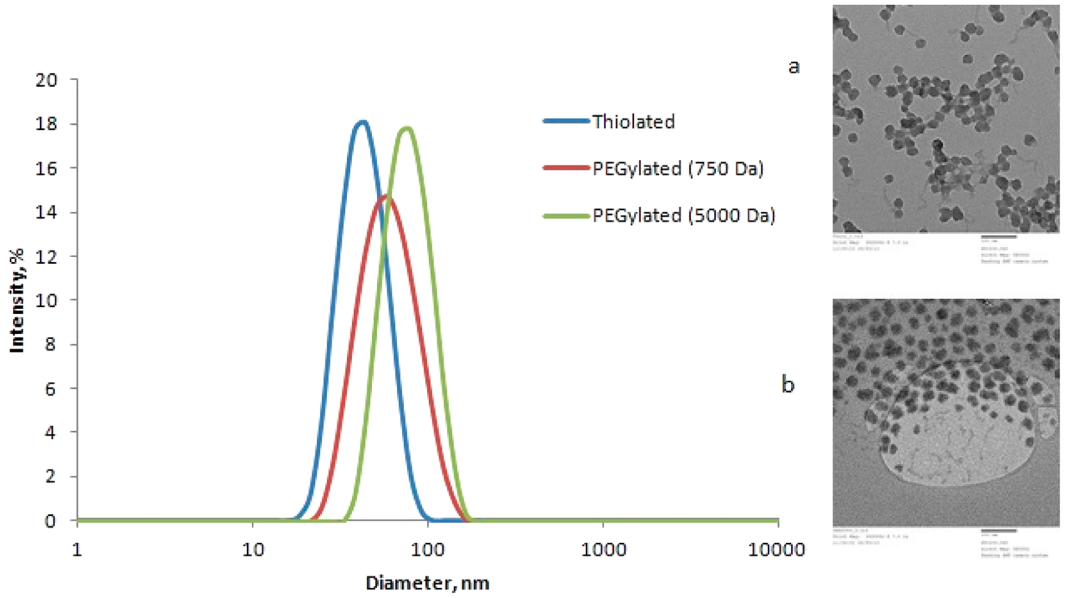

Figure 1. Size distribution of fluorescently labeled thiolated and PEGylated nanoparticles. The mean particle diameters are 44 ± 2, 52 ± 1, and 68 ± 2 nm for thiolated and PEGylated (750 and 5000 Da), respectively. (Insets) TEM images of (a) thiolated and (b) 5000 Da PEGylated nanoparticles. The size bar is 100 nm.

The polydispersity of spheres is determined from a Shultz distribution.[14]

Radius values from DLS and TEM were used as guides for the SANS analysis. In all cases, absolute intensity and scale factor checks were made to ensure that the values obtained were physically realistic.

Fluorometry. Fluorescence spectra were recorded for fluorescently labeled nanoparticles using an FP-6200 spectrofluorometer (Jasco, U.K.) over the wavelength range of 555−700 nm (λ_{ex} = 546 nm).

Preparation of Polymer Solutions. Aqueous solutions of HEC, PAA, PEO, and PVP were prepared by dispersing the required amounts of polymer powders in deionized water and stirring them overnight at room temperature until complete dissolution. Solutions of PAA with the same viscosity at different pH values were prepared; a 0.015% w/v solution of PAA in deionized water gave a pH of 3.98 and a viscosity of 5.10 cP. A PAA solution at higher pH (pH 5.04) was prepared by adding a drop of 1 M NaOH to the original PAA solution (0.015% w/v, pH 3.98, 5.10 cP). The viscosity of this new solution was measured and was unaffected, remaining at 5.10 cP. A PAA solution at lower pH (pH 2.98) was prepared by producing a series of solutions at differing concentrations (0.02 to 0.14% w/v) whose pH and viscosity were recorded; a 0.13% w/v PAA solution whose pH was adjusted to 2.98 by adding 1 M HCl gave a viscosity of 5.10 cP.

Viscometry. The viscosity of four polymer aqueous solutions (HEC, PAA, PEO, and PVP) over the range of 0.1−5 w/v% was measured using a Brookfield DV-II+Pro viscometer (Brookfield Engineering Laboratories, Inc, USA) at 25 °C with a S62 spindle (LV series) at 60 rpm. The data were used to prepare polymer solutions of the same viscosity (5.10 cP) for diffusion experiments. The relative viscosity of aqueous HEC, PVP, and PEO solutions was determined using an AVS 470 CAMLAB Serving Science viscometry system (Schott Instruments) with a Schott Gerate capillary viscometer at 25 °C. The polymer solutions were prepared at five different concentrations (0.5, 0.6, 0.7, 0.8, and 1 mg/mL) in deionized water. Twenty milliliters of each solution or deionized water was placed into the capillary viscometer and allowed to reach temperature equilibrium for 5 min. The flow time of each sample was measured five times, and the mean viscosity ± SD was calculated for polymer solutions ($t_{polymer}$) and the solvent ($t_{solvent}$). The relative viscosity of each individual polymer solution was calculated according to

$$\eta_{rel} = \frac{t_{polymer}}{t_{solvent}}$$

The specific viscosity (η_{sp}) was calculated: $\eta_{sp} = \eta_{rel} - 1$. The graph of $\eta_{sp}/C_{polymer}$ versus polymer concentration ($C_{polymer}$) was plotted, and the intrinsic viscosity $[\eta]$ was determined by extrapolating to $C_{polymer}$ = 0. The overlap concentration of the polymer was calculated using the following relationship:

$$C^* = \frac{1}{[\eta]}$$

Diffusion Coefficient Measurements. The diffusion coefficients of fluorescently labeled nanoparticles were measured using a NanoSight LM10HSGF system fitted with a syringe pump. The system was equipped with a scientific CMOS camera, a 532 nm laser with temperature control, and a 565 nm long-pass filter for fluorescent particle analysis. NTA 2.3 analytical software was used to capture and analyze three 60 s videos from each sample; the camera level was set to 16, and the temperature was set to 25 °C throughout. The ideal concentration of nanoparticles for NTA measurement should be within 1×10^8−25×10^8 particles/mL. All samples were diluted 10 000-fold with the relevant polymer solutions prior to analysis to give 4×10^{-5} mg/mL nanoparticle dispersions. A syringe pump drove the sample through the sample chamber to minimize fluorophore photobleaching. No macroscopic phase separation was observed in any nanoparticle dispersion in solutions of polymers. For analysis, a multiple detection threshold, automatic blur, automatic minimum track length, and automatic minimum expected particle size were used, according to the manufacturer's recommendations.

Ellman's Assay. The number of SH groups on thiolated and PEGylated nanoparticles was determined by Ellman's assay.[9,10] Freeze-dried nanoparticles (0.2−0.3 mg) were allowed to hydrate in 500 μL of phosphate buffer solution (0.5 mol/L, pH 8). Then, 500 μL of DTNB solution (0.3 mg/mL in phosphate buffer) was added to 500 μL of a nanoparticle dispersion, and the reaction was allowed to proceed for 2 h in the dark. The nanoparticle dispersion was then centrifuged for 10 min at 13 000 rpm (Sanyo, MSE Micro Centaur), 200 μL aliquots of supernatant were placed in 96-well microtiter plates, and absorbance was measured at 420 nm (Epoch Microplate Spectrophotometer, BioTek Instruments, USA). The thiol-group contents were calculated from a calibration curve prepared using cysteine hydrochloride solutions over the concentration range of 25−175 μmol/L.

Statistical Analysis. Statistical analysis of diffusion coefficients in water and four polymer solutions used a one-way anova test. The

dx.doi.org/10.1021/la4029035 | Langmuir 2014, 30, 308−317

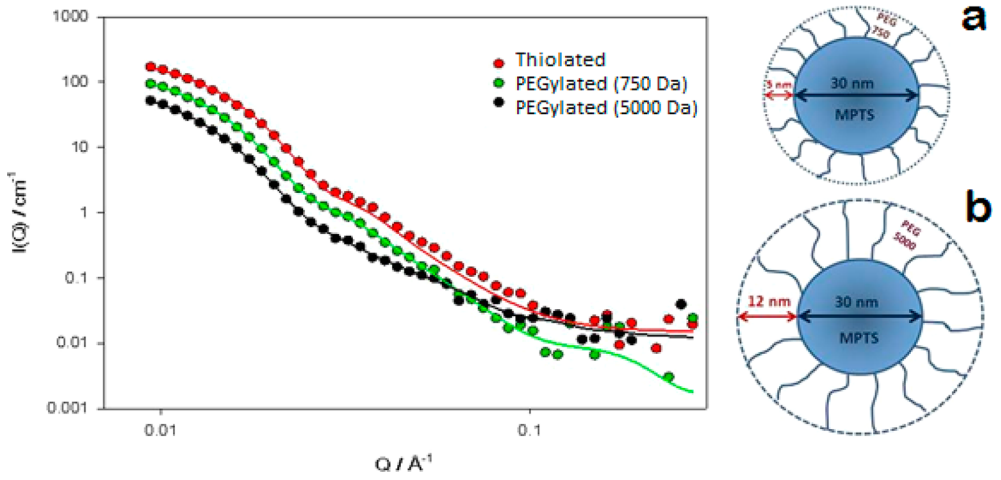

Figure 2. SANS data for thiolated MPTS nanoparticles and their PEGylated derivatives with initial fits through the data (PEGylation with 750 and 5000 Da PEG). (Insets) Sketches of nanoparticles consisting of an MPTS core and (a)750 or (b) 5000 Da PEG shells.

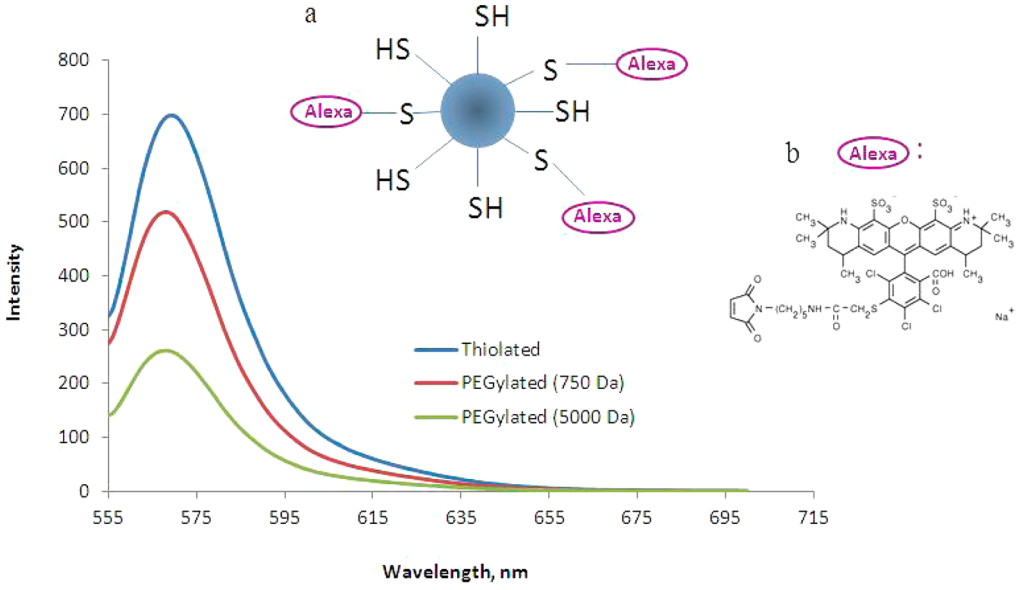

Figure 3. Fluorescence spectra of thiolated and PEGylated (750 and 5000 Da) nanoparticles. The concentration of nanoparticles in all aqueous dispersion is 3.2 mg/mL. (Insets) Schematic structure of thiolated nanoparticles: (a) fluorescently labeled with Alexa 546 maleimide dye and (b) the chemical structure of Alexa 546 maleimide. Note that this structure does not show the quantitative content of Alexa with respect to SH groups in the nanoparticles.

difference between the measured values was considered to be significant for $p < 0.05$.

RESULTS AND DISCUSSION

Synthesis and Characterization of Nanoparticles. Previously, we reported a novel synthesis of 55 ± 4 nm thiolated nanoparticles by the self-condensation of (3-mercaptopropyl)trimethoxysilane (MPTS) in dimethyl sulfoxide.[9,10] Here, synthesis followed a similar protocol, but the reaction mixture was additionally bubbled with atmospheric air, which accelerates and ensures further cross-linking via disulfide bond formation during particle formation as we previously reported.[9,10] This protocol resulted in 44 ± 1 nm nanoparticles as measured by dynamic light scattering.

The thiolated nanoparticles were PEGylated by reacting with 750 and 5000 Da methoxypoly(ethylene glycol) maleimide. The size of both thiolated and PEGylated nanoparticles was determined using dynamic light scattering (DLS) and transmission electron microscopy (TEM) (Figure 1).

Both DLS and TEM demonstrate an expected increase in the size of nanoparticles after PEGylation because of the PEG corona on their surfaces. Thiolated nanoparticles tend to aggregate because of the formation of interparticle disulfide bridges[9,10] whereas PEGylation reduces aggregation. The decreased number of thiol groups after PEGylation was confirmed by Raman spectroscopy (data not shown) and quantified by Ellman's assay from 249 ± 30 μmol/g for thiolated nanoparticles to 89 ± 4 and 78 ± 5 μmol/g for 750 and 5000 Da PEGylated nanoparticles, respectively.

Small-Angle Neutron Scattering. Small-angle neutron scattering (SANS) is a powerful technique to characterize the structure of polymers and complex nanomaterials in solutions.[15,16] Previously SANS was used to study interactions between silica nanoparticles and poly(ethylene oxide).[17,18] Here, SANS was employed to determine the structural features

dx.doi.org/10.1021/la4029035 | Langmuir 2014, 30, 308−317

of both thiolated and PEG-coated nanoparticles. Figure 2 shows SANS scattering patterns and the schematic structures of PEGylated nanoparticles. The thiolated nanoparticles were modeled using the spherical form factor as described above. A good fit and agreement between calculated and fitted scale factors was achieved with a particle diameter of 30 nm and a polydispersity of 0.2. The discrepancy between the particle size measured by dynamic light scattering (44 ± 2 nm) and by SANS (30 ± 1 nm) is related to the particle hydration layer to which SANS is insensitive. The thickness of hydration layers on silica surfaces reported in the literature is around 4−10 nm.[19−21] Both PEGylated nanoparticles were initially modeled with only a spherical form factor, and although the particle size increased as expected, the goodness of fit and scale factor comparisons improved with the addition of the core−shell variables to the model. It was found that the particles were composed of a 30 nm spherical core (which was in good agreement with the core particle size found from the thiolated particle fit) and a hydrated PEG shell that is 5 and 12 nm thick for PEGylation with 750 and 5000 Da PEG, respectively.

Fluorescent Labeling of Nanoparticles. The thiolated nanoparticles were fluorescently labeled by reaction with Alexa Fluor 546 C5 maleimide. Dynamic light scattering analysis of thiolated nanoparticles established that there is no significant difference in size distributions before and after fluorescent labeling (Figure S1, Supporting Information). Some fluorescently labeled samples were additionally PEGylated. Figure 3 shows a higher fluorescence intensity in the spectrum of labeled thiolated nanoparticles compared to that of the PEGylated particles. The reduced fluorescence intensity on PEGylation is likely to be due to screening effects resulting from nonfluorescent PEG shells; the larger PEG molecular weight provided the lowest intensity because screening with PEG 5000 Da is more efficient than with PEG 750 Da.

Diffusion Studies of Thiolated and PEGylated Nanoparticles in Aqueous Polymer Solutions. NanoSight's nanoparticle tracking analysis (NTA) can be used to characterize the dimensions of nanomaterials in liquid media (Newtonian fluids); the Brownian motion of individual nanoparticles is tracked, and through the analysis of their diffusion characteristics, the particle size and size distributions can be calculated using the Stokes−Einstein equation. NTA has previously been accurately used to size various nanomaterials including polymeric and metal nanoparticles, micelles, emulsions, viruses, and other colloids.[22−26] NTA is a more accurate sizing technique than DLS when polydisperse samples are used because the motion of individual particles is tracked. Although DLS does not track individual particles, it does evaluate light scattering from particles in a sample simultaneously.

NanoSight's fluorescence versions of the LM Series instrument also allow the tracking of fluorescent nanoparticles that are dispersed in complex nonfluorescent media. This technique is similar to single/multiple particle tracking methods that previously have been used as powerful tools to examine the diffusion and interactions of nanoparticles.[27−29]

In the present work, we used the fluorescence version of NanoSight's LM Series instrument to evaluate the diffusional characteristics of our nanoparticles in solutions of different water-soluble polymers: poly(acrylic acid) (PAA, 450 000 Da), poly(ethylene oxide) (PEO, 1 000 000 Da), 2-hydroxyethylcellulose (HEC, 90 000 Da), and poly(vinylpyrrolidone) (PVP, 360 000 Da). These polymers were selected as well-characterized materials that are widely used in pharmaceutical and cosmetic formulations as stabilizers, gelling agents, and lubricants[30] and importantly provide different hydrogen-bonding capabilities: PAA is a classical proton-donating polymer, PEO and PVP can act only as proton acceptors, and HEC can exhibit both proton-donating and proton-accepting activities. The proton-accepting ability of these polymers typically decreases in the order PVP > PEO > HEC, as confirmed by their interactions with PAA to form hydrogen-bonded interpolymer complexes in aqueous solutions.[31]

Initially, these water-soluble polymers were studied viscometrically to establish optimal concentrations resulting in solutions of equal viscosity (Figure S2, Supporting Information). Aqueous solutions of the polymers with a viscosity of 5.10 ± 0.05 cP were prepared for the diffusion studies, corresponding to polymer concentrations of 0.015 w/v % PAA, 0.4 w/v % PVP, 0.08 w/v % PEO, and 0.4 w/v % HEC. The pH values for these solutions were 3.98, 5.77, 4.19, and 6.10 for PAA, HEC, PVP and PEO, respectively. The pH of polymer solutions did not change significantly upon addition of nanoparticles. Further viscometric experiments (Figure S3, Supporting Information) demonstrated that the concentrations of PVP, PEO, and HEC used in this work were below the overlap concentration (C^*) (i.e., the solutions used were in the dilute concentration regime).

A study of nanoparticle diffusion in solutions of different water-soluble polymers at equal viscosity allows the chemical nature of the liquid medium on nanoparticle diffusivity to be explored. Figure 4 shows typical diffusion coefficient distributions of thiolated and selected PEGylated nanoparticles in deionized water and in solutions of PAA, PVP, PEO, and HEC, recorded using a NanoSight LM10-HS optical microscope with a Nanosight LM14 laser unit. An example video and the diffusion coefficient distributions recorded for other PEGylated nanoparticles can be found in the Supporting Information (Figure S4).

According to NanoSight's technical literature,[26] an accurate estimation of diffusion coefficients using NTA relies on the instrument's ability to track any given particle's Brownian motion trajectory for a sufficient number of steps to generate an average step-length value. Because of the small depth of scattering volume, smaller and faster-moving particles in particular can often be tracked for a limited period of time (<10 frames = 0.3 s at 30 fps). This results in artificial broadening of the measured distributions, but the mean values of diffusion coefficients are claimed to be very accurate. In our case, faster-moving particles indeed show broader diffusion coefficient distributions. We based our comparison of the diffusivity of nanoparticles not only on the diffusion coefficient (D) distributions but also on the mean D values reported by the instrument. Different particles' trajectories have also been compared to ensure the validity of conclusions drawn from NTA measurements. Some example particle trajectories can be found in the Supporting Information (Figure S5).

Diffusion coefficients of spherical nanoparticles have been reported using diffusion NMR techniques.[32] Typically, these studies report single (mean) D values rather than distributions for a given type of nanoparticle. Considering that nanoparticles are typically polydisperse, a distribution of diffusion coefficients more accurately reflects the nanoparticle sample properties and is a significant advantage of the nanoparticle tracking analysis technique.

dx.doi.org/10.1021/la4029035 | Langmuir 2014, 30, 308−317

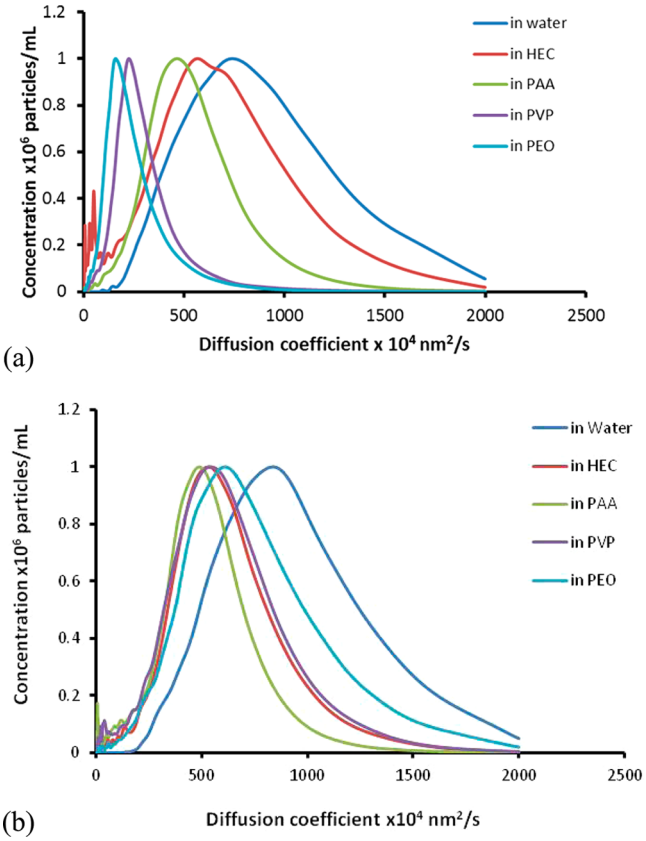

Figure 4. Diffusion coefficient distributions of (a) thiolated and (b) PEGylated 5000 Da nanoparticles in water and aqueous polymer solutions at 5.10 cP.

Table 1 summarizes the mean diffusion coefficients for thiolated and PEGylated nanoparticles measured with the NanoSight NTA and compares them with calculated values using the Stokes–Einstein equation. The highest diffusion coefficients for thiolated and PEGylated nanoparticles were registered upon dispersion in deionized water, which was expected because this medium has a much lower viscosity (0.89 cP) than solutions of polymers (5.10 cP). The diffusion coefficient recorded for thiolated nanoparticles in deionized water ($731 \pm 40 \times 10^4$ nm^2/s) was lower than the value calculated using the Stokes–Einstein equation (1115×10^4 nm^2/s). This discrepancy could be related to the interaction of nanoparticles with water molecules and the formation of a hydration layer. PEGylated particles were expected to have lower diffusion coefficients in distilled water when compared to their parent thiolated particles because of their larger sizes. However, the experimental results show surprisingly higher values for the diffusion coefficients: $(906 \pm 89) \times 10^4$ and $(834 \pm 29) \times 10^4$ nm^2/s for the nanoparticles PEGylated with 750 and 5000 Da PEG, respectively; these differences between PEGylated and thiolated particles in water are statistically significant ($p < 0.001$ and $p < 0.01$ for PEG 750 and 5000 Da, respectively). The reasons for this unusual enhancement in the diffusivity of PEGylated nanoparticles in water are not clear, but it is likely that the PEG chains provide additional "lubrication" that facilitates their mobility in water.

As expected, the coefficients recorded for the nanoparticles in polymer solutions were all significantly ($p < 0.001$) lower compared to their diffusion in deionized water as a result of the increased viscosity of the medium. However, a comparison of the diffusion coefficients with the values calculated using the Stokes–Einstein equation reveals that the experimental data are several times greater than the predicted results. This discrepancy illustrates that the Stokes–Einstein relationship is not valid for predicting diffusion coefficients of these nanoparticles in polymer solutions, in agreement with recent literature reports.[33,34] Deviations from the Stokes–Einstein

Table 1. Dimensions and Diffusion Characteristics of Thiolated and PEGylated Nanoparticles

nanoparticles	nanoparticle size, nm (DLS)	medium	medium viscosity (cP)	diffusion coefficient, $\times 10^4$ nm^2/s (Stokes–Einstein equation)	diffusion coefficient, $\times 10^4$ nm^2/s (NanoSight)
thiolated	44 ± 2	water	0.89	1115	731 ± 40
thiolated	44 ± 2	HEC	5.10	195	593 ± 55
thiolated	44 ± 2	PAA	5.10	195	461 ± 28
thiolated	44 ± 2	PVP	5.10	195	238 ± 30
thiolated	44 ± 2	PEO	5.10	195	172 ± 44
PEGylated (750 Da)	52 ± 1	water	0.89	943	906 ± 89
PEGylated (750 Da)	52 ± 1	HEC	5.10	165	614 ± 51
PEGylated (750 Da)	52 ± 1	PAA	5.10	165	553 ± 23
PEGylated (750 Da)	52 ± 1	PVP	5.10	165	626 ± 46
PEGylated (750 Da)	52 ± 1	PEO	5.10	165	721 ± 45
PEGylated (5000 Da)	68 ± 2	water	0.89	721	834 ± 29
PEGylated (5000 Da)	68 ± 2	HEC	5.10	126	534 ± 21
PEGylated (5000 Da)	68 ± 2	PAA	5.10	126	487 ± 6
PEGylated (5000 Da)	68 ± 2	PVP	5.10	126	547 ± 21
PEGylated (5000 Da)	68 ± 2	PEO	5.10	126	614 ± 27

dx.doi.org/10.1021/la4029035 | *Langmuir* 2014, 30, 308–317

relationship were previously observed when particle radii (R) were smaller or comparable to the radius of gyration (R_g) of polymers present in a liquid medium (solution or melt). Indeed, the R values measured for our nanoparticles using SANS ($^1/_2 \times$ particle diameters from Figure 2: 15, 17.5, and 21 nm for thiolated and 750 and 5000 Da PEGylated, respectively) are smaller than the R_g reported for PEO (25−30 nm for 600 000 Da PEO in D_2O[35] and 48.5 nm for 417 kDa PEO in water[36]) and PVP (42.5 nm for 541 kDa PVP[36]), which explains the discrepancy between the experimentally measured and theoretical values.

The measured diffusivity for thiolated nanoparticles in polymeric solutions was greatest in HEC [$(593 \pm 55) \times 10^4$ nm^2/s] as a result of the absence of specific interactions with this polymer. A significantly lower diffusion coefficient of $(461 \pm 28) \times 10^4$ nm^2/s was recorded for these nanoparticles in PAA ($p \leq 0.001$), demonstrating the attraction between thiolated silica surface and PAA macromolecules, hampering nanoparticle diffusion. These results are in contrast to data from Drechsler et al.,[37] who studied the interactions between micronized silica spheres and PAA over a wide range of pH values (2.5−9.2) and observed only repulsive behavior; this discrepancy may result from the different surface chemistry of our particles (i.e., the presence of thiol groups on their surface).

An even greater reduction in the diffusion coefficients was observed in PEO and PVP solutions, giving $(172 \pm 44) \times 10^4$ and $(238 \pm 30) \times 10^4$ nm^2/s, respectively. This dramatic reduction in the diffusivity observed for the thiolated nanoparticles is due to strong hydrogen bonding between −Si−OH groups on the nanoparticle surface (proton-donating properties) and proton-accepting oxygen in the structure of PEO and PVP. The strong interactions of silica nanoparticles with PEO[17−21,38] and PVP[39] have been reported previously.

The PEGylated nanoparticles display dramatically different diffusivity in polymer solutions compared to their thiolated counterpart. The greatest diffusion coefficients were recorded for the nanoparticles in PEO solutions [$(721 \pm 45) \times 10^4$ and $(614 \pm 27) \times 10^4$ nm^2/s for PEGylation with 750 and 5000 Da PEG, respectively]. This is logical because no interaction is expected between PEGylated surfaces and PEO macromolecules as a result of their chemical similarity. The diffusivity of PEGylated nanoparticles in solutions of PVP and HEC was lower compared to that of PEO [e.g., $(626 \pm 46) \times 10^4$ and $(614 \pm 51) \times 10^4$ nm^2/s for PEG 750 Da in PVP and HEC, respectively), indicating the presence of very weak interactions; there was also no significant difference between the diffusion coefficients for the nanoparticles in HEC and PVP ($p > 0.05$). PEO, PVP, and HEC predominantly exhibit proton-accepting properties and essentially do not interact with proton-accepting PEG present on the surface of PEGylated nanoparticles. A significant ($p < 0.01$) reduction in the diffusivity was observed for PEGylated nanoparticles in solutions of PAA [$(553 \pm 23) \times 10^4$ and $(487 \pm 6) \times 10^4$ nm^2/s for 750 and 5000 Da PEG, respectively] compared to PEO, PVP, and HEC. This ability of PAA to hamper the diffusivity of PEGylated nanoparticles is probably related to complex formation between PAA and PEG via hydrogen bonding. A more pronounced reduction in diffusivity is observed for the nanoparticles PEGylated with larger-molecular-weight PEG (5000 Da), which is also consistent with the complexation hypothesis because larger macromolecules are expected to form stronger interpolymer complexes.[40] Typically, complexation between PAA and PEG or PEO is observed under acidic conditions ($pH_{crit} < 4.0$),[41] and we previously reported the aggregation of PEGylated silica nanoparticles caused by the addition of PAA at pH 2.96.[10] However, the pH of the PAA solution used in these experiments was 3.98, which is very close to the critical pH of complex formation between PAA and PEO. Hydrogen bonding interactions under these conditions are still possible, but they are not as strong as in the case of thiolated nanoparticles dispersed in PVP or PEO solutions (where a more dramatic drop in diffusivity is observed).

The diffusivity of nanoparticles in solutions of polymers also depends on the viscosity, in accordance with the Stokes−Einstein equation. Experiments performed in more concentrated polymer solutions (viscosity 9.90 cP) revealed a dramatic reduction in nanoparticle diffusion in all cases. For example, the diffusion coefficients recorded in solutions of HEC (9.90 cP) were $(458 \pm 39) \times 10^4$, $(421 \pm 17) \times 10^4$, and $(390 \pm 16) \times 10^4$ nm^2/s for thiolated nanoparticles and PEGylated nanoparticles with 750 and 5000 Da PEG, respectively. Similar trends were observed for the diffusion of nanoparticles in solutions of PVP and PAA (data not shown).

To confirm further that the reduction in the diffusivity of nanoparticles is related to their specific interactions with macromolecules present in polymer solutions, experiments were conducted probing the effect of pH on the diffusivity in solutions of poly(acrylic acid) (Table 2).

Table 2. Effect of pH on the Diffusivity of Thiolated and PEGylated Nanoparticles in Solutions of Poly(acrylic acid)

	viscosity of PAA, cP[a]	pH of PAA	diffusion coefficient, $\times 10^4$ nm^2/s (NanoSight)
thiolated	5.10	2.98	489 ± 25
thiolated	5.10	3.98	461 ± 28
thiolated	5.10	5.04	452 ± 74
PEGylated (750 Da)	5.10	2.98	407 ± 51
PEGylated (750 Da)	5.10	3.98	553 ± 23
PEGylated (750 Da)	5.10	5.04	574 ± 65
PEGylated (5000 Da)	5.10	2.98	264 ± 39
PEGylated (5000 Da)	5.10	3.98	487 ± 7
PEGylated (5000 Da)	5.10	5.04	534 ± 41

[a]The same viscosity of PAA solutions at different pH values was achieved by varying the polymer concentrations.

The diffusion coefficients of the thiolated nanoparticles in PAA solutions do not show a significant dependence on pH ($p > 0.05$) and remain within $(452−489) \times 10^4$ nm^2/s. This is consistent with the report by Drechsler et al.[37] that reported the absence of attractive interactions between silica and PAA. However, our data suggests that some weak interactions between PAA and thiolated silica remain, as evidenced by lower D values when compared to nanoparticle diffusion in HEC.

However, the diffusivity of PEGylated nanoparticles was clearly pH-dependent: a significant reduction in the diffusion coefficients was observed at pH 2.98 for both PEG 750 Da and PEG 5000 Da ($p \leq 0.001$). Moreover, the effect of pH is more pronounced in the case of the nanoparticles PEGylated with larger-molecular-weight PEG (5000 Da): a pH decrease from 5.04 to 2.98 results in a significant halving of the diffusion coefficient from $(534 \pm 41) \times 10^4$ nm^2/s to $(264 \pm 39) \times 10^4$

dx.doi.org/10.1021/la4029035 | Langmuir 2014, 30, 308−317

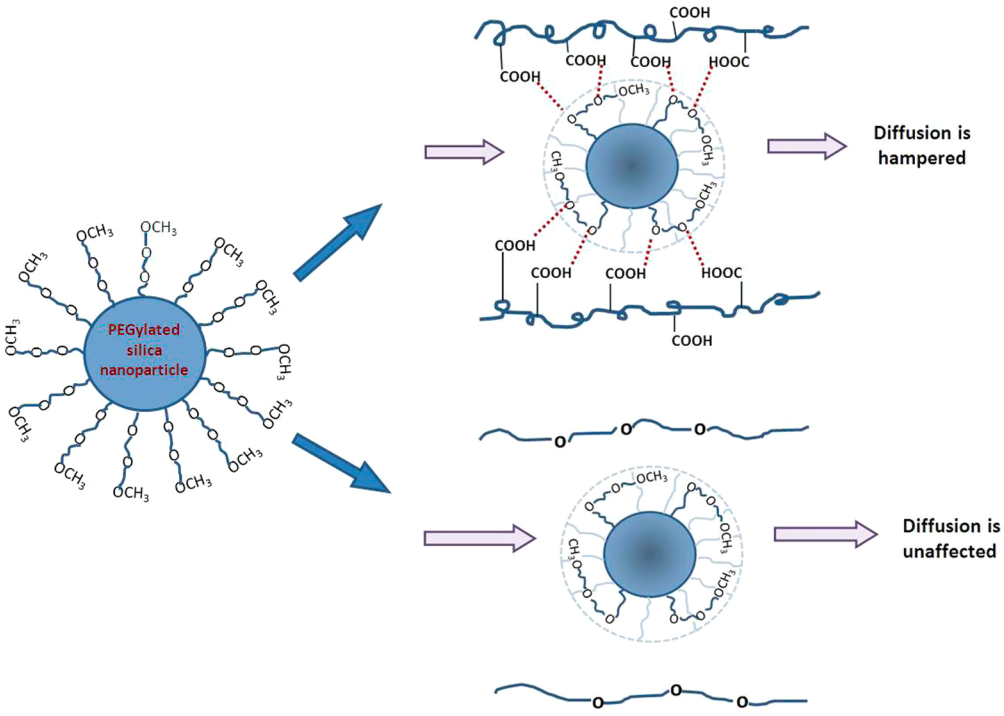

Figure 5. Illustration of the influence on diffusivity of specific interactions between nanoparticle surfaces (PEGylated) with polymeric solutions (e.g., PAA or PEO).

nm^2/s ($p \leq 0.001$). This observation is in good agreement with our previous report on the effect of pH on the complexation between PAA and PEO.[41] Hydrogen bonding between these polymers is typically observed at pH < 4.0 and is not possible at higher pH values. The more pronounced pH effect for the larger-molecular-weight PEG is related to the minimal critical chain length of this polymer, above which complexation is possible.[40]

Comparing the diffusion coefficients of thiolated nanoparticles with the nanoparticles coated with PEG 750 at pH 5.04 reveals a significant increase in diffusivity on PEGylation ($p \leq 0.001$). Under these pH conditions, hydrogen-bonding between PEG and PAA is not possible and the PEGylated nanoparticles show enhanced diffusivity compared to their thiolated counterparts despite their larger size. This is consistent with their enhanced diffusivity in pure water discussed previously and can be explained by some "lubricating" effects provided by the PEGylated surface. The facilitated transport of PEGylated nanoparticles is also in a good agreement with recent reports by Hanes et al.[7,8] The impact of interactions between PEGylated particles and PAA on diffusivity is illustrated in Figure 5; strong interactions may hamper diffusion whereas if these interactions are very weak or absent then diffusion will be unaffected and will be predominantly governed by the particle size and medium viscosity.

CONCLUSIONS

For the first time, the diffusion of nanoparticles has been studied in different polymer solutions using NanoSight nanoparticle tracking analysis with fluorescence detection. Our studies reveal that three main factors affect diffusion: the size of the nanoparticles, the medium viscosity and the presence of specific interactions between nanoparticles, and the components of the liquid medium. The presence of strong attractive interactions such as hydrogen bonding between the nanoparticles and macromolecules present in solutions can hamper their diffusion.

Coating nanoparticles with PEG can enhance their diffusivity in water, despite an increase in their dimensions. The physics of this effect is currently not fully clear but may be related to the lubricating properties of this coating.

Investigating the factors affecting the diffusivity of nanomaterials in complex mixtures containing polymers or biopolymers provides the further understanding necessary for the development of novel nanomedicines for drug delivery, complex cosmetics, glue, and paint formulations. Nanoparticles that strongly interact with biopolymers present in a biological gel such as mucus may be trapped in its network and thus may be unable to permeate the matrix to reach target epithelial cells.

ASSOCIATED CONTENT

Supporting Information

Dynamic light scattering data of nanoparticles before and after fluorescent labeling, viscosity of different polymer solutions, intrinsic viscosities to work out overlap concentrations (C^*), diffusion coefficient distributions for PEGylated 750 Da nanoparticles in water and aqueous polymer solutions, and example nanoparticle tracks. This material is available free of charge via the Internet at http://pubs.acs.org.

AUTHOR INFORMATION

Corresponding Author

*E-mail: v.khutoryanskiy@reading.ac.uk,. Tel: +44 (0) 118 373 6119.

Notes

The authors declare no competing financial interest.

■ ACKNOWLEDGMENTS

The help of Dr. P. Harris (Centre for Advanced Microscopy) with TEM experiments is greatly appreciated. The Chemical Analysis Facility at the University of Reading is acknowledged for providing access to a Raman spectrometer. We are grateful to STFC for providing access to SANS beam time as part of SANS Xpress (proposal 1 293 003).

■ REFERENCES

(1) Einstein, A. On the movement of small particles suspended in stationary liquids required by the molecular-kinetic theory of heat. *Ann. Phys.* **1905**, *17*, 549−560.
(2) Squires, T. M.; Mason, T. G. Fluid mechanics of microrheology. *Annual. Rev. Fluid Mech.* **2010**, *42*, 413−438.
(3) Chilvers, M. A.; O'Callaghan, C. Local mucociliary defense mechanisms. *Paediatr. Respir. Rev.* **2000**, *1*, 27−34.
(4) Treacy, K.; Tunney, M.; Elborn, J. S.; Bradley, J. M. Mucociliary clearance in cystic fibrosis: physiology and pharmacological treatments. *Paediatr. Child Health* **2011**, *21*, 425−430.
(5) Sanders, N. N.; Peeters, L.; Lentacker, I.; Demeester, J.; De Smedt, S. C. Wanted and unwanted properties of surface PEGylated nucleic acid nanoparticles in ocular gene transfer. *J. Controlled Release* **2007**, *122*, 226−235.
(6) Das Neves, J.; Amiji, M.; Sarmento, B. Mucoadhesive nanosystems for vaginal microbicide development: friend or foe? *Nanomed. Nanobiotechnol.* **2011**, *3*, 389−399.
(7) Lai, S. K.; O'Hanlon, D. E.; Harrold, S.; Man, S. T.; Wang, Y. Y.; Cone, R.; Hanes, J. Rapid transport of large polymeric nanoparticles in fresh undiluted human mucus. *Proc. Natl. Acad. Sci. U.S.A.* **2007**, *104*, 1482−1487.
(8) Wang, Y. Y.; Lai, S. K.; Suk, J. S.; Pace, A.; Cone, R.; Hanes, J. Addressing the PEG mucoadhesivity paradox to engineer nanoparticles that "slip" through the human mucus barrier. *Angew. Chem., Int. Ed. Engl.* **2008**, *47*, 9726−9729.
(9) Irmukhametova, G. S.; Mun, G. A.; Khutoryanskiy, V. V. Thiolated mucoadhesive and PEGylated nonmucoadhesive organosilica nanoparticles from 3-mercaptopropyltrimethoxysilane. *Langmuir* **2011**, *27*, 9551−9556.
(10) Irmukhametova, G. S.; Fraser, B. J.; Keddie, J. L.; Mun, G. A.; Khutoryanskiy, V. V. The hydrogen bonding-driven self-assembly of PEGylated organosilica nanoparticles with poly(acrylic acid) in aqueous solutions and in layer-by-layer deposition at solid surfaces. *Langmuir* **2012**, *28*, 299−306.
(11) Heenan, R. K.; Penfold, J.; King, S. M. SANS at pulsed neutron sources: present and future prospects. *J. Appl. Crystallogr.* **1997**, *30*, 1140−1147.
(12) http://mantidproject.org
(13) Wignall, G. D.; Bates, F. S. Absolute calibration of small-angle neutron scattering data. *J. Appl. Crystallogr.* **1987**, *20*, 28−40.
(14) Kotlarchyk, M.; Chen, S.-H. Analysis of small-angle neutron-scattering spectra from polydisperse interacting colloids. *J. Chem. Phys.* **1983**, *79*, 2461−2469.
(15) Horkay, F.; Hammouda, B. SANS from model synthetic and biopolymer solutions. *Colloid Polym. Sci.* **2008**, *286*, 611−620.
(16) Blin, J. L.; Imperor-Clerc, M. Mechanism of self-assembly in the synthesis of silica mesoporous materials: in situ studies by X-ray and neutron scattering. *Chem. Soc. Rev.* **2013**, *42*, 4071−4082.
(17) Qiu, D.; Dreiss, C. A.; Cosgrove, T. Small-angle neutron scattering study of concentrated colloidal dispersions: the interparticle interactions between sterically stabilized particles. *Langmuir* **2005**, *21*, 9964−9969.
(18) Joksinovic, R.; Prevost, S.; Schweins, R.; Appavou, M.-S.; Gradzielski, M. Interactions of silica nanoparticles with poly(ethylene oxide) and poly(acrylic acid): effect of the polymer molecular weight and of the surface charge. *J. Colloid Interface Sci.* **2013**, *394*, 85−93.
(19) Nalaskowski, J.; Drelich, J.; Hupka, J.; Miller, J. D. Adhesion between hydrocarbon particles and silica surfaces with different degrees of hydration as determined by AFM colloidal probe technique. *Langmuir* **2003**, *19*, 5311−5317.
(20) Barnette, A. L.; Kim, S. H. Coadsorption of n-propanol and water on SiO_2: study of thickness, composition, and structure of binary adsorbate layer using attenuated total reflection infrared (ATR-IR) and sum frequency generation (SFG) vibration spectroscopy. *J. Phys. Chem. C* **2012**, *116*, 9909−9916.
(21) He, L.; Hu, Y.; Yin, Y. Determination of salvation layer thickness by a magnetophotonic approach. *ACS Nano* **2012**, *6*, 4196−4202.
(22) Tixier, T.; Heppenstall-Butler, M.; Terentjev, E. M. Spontaneous size selection in cholesteric and nematic emulsions. *Langmuir* **2006**, *22*, 2365−2370.
(23) Zhunuspayev, D. E.; Mun, G. A.; Hole, P.; Khutoryanskiy, V. V. Temperature-responsive properties and drug solubilization capacity of amphiphilic copolymers based on N-vinylpyrrolidone and vinyl propyl ether. *Langmuir* **2008**, *24*, 13742−13747.
(24) Steinmetz, N. F.; Shah, S. N.; Barclay, J. E.; Rallapalli, G.; Lomonossoff, G. P.; Evans, D. J. Virus-templated silica nanoparticles. *Small* **2009**, *5*, 813−816.
(25) Aljabali, A. A. A.; Barclay, J. E.; Lomonossoff, G. P.; Evans, D. J. Virus templated metallic nanoparticles. *Nanoscale* **2010**, *2*, 2596−2600.
(26) Carr, B.; Wright, M. Nanoparticle Tracking Analysis: A Review of Applications and Usage 2010−2012, ©NanoSight Ltd 2013, p.188.
(27) Suh, J.; Dawson, M.; Hanes, J. Real-time multiple-particle tracking: applications to drug and gene delivery. *Adv. Drug Delivery Rev.* **2005**, *57*, 63−78.
(28) Rife, J. C.; Long, J. P.; Wilkinson, J.; Whitman, L. J. Particle tracking single protein-functionalized quantum dot diffusion and binding at silica surfaces. *Langmuir* **2009**, *25*, 3509−3518.
(29) Filipe, V.; Poole, R.; Kutscher, M.; Forier, K.; Braeckmans, K.; Jiskoot, W. Fluorescence single particle tracking for the characterization of submicron protein aggregates in biological fluids and complex formulations. *Pharm. Res.* **2011**, *28*, 1112−1120.
(30) Williams, P. A. *Handbook of Industrial Water Soluble Polymers*; Blackwell Publishing: Oxford, U.K., 2007.
(31) Khutoryanskiy, V. V.; Staikos, G. *Hydrogen-Bonded Interpolymer Complexes*; World Scientific: Singapore, 2009; p 366.
(32) Occhipinti, P.; Griffiths, P. C. Quantifying diffusion in mucosal systems by pulsed-gradient spin-echo NMR. *Adv. Drug Delivery Rev.* **2008**, *60*, 1570−1582.
(33) Tuteja, A.; Mackay, M. E.; Narayanan, S.; Asokan, S.; Wong, M. S. Breakdown of the continuum Stokes−Einstein relation for nanoparticle diffusion. *Nano Lett.* **2007**, *7*, 1276−1281.
(34) Liu, J.; Cao, D.; Zhang, L. Molecular dynamics study on nanoparticle diffusion in polymer melts: a test of the Stokes−Einstein law. *J. Phys. Chem. C* **2008**, *112*, 6653−6661.
(35) Branca, C.; Magazu, S.; Maisano, G.; Migliardo, F.; Migliardo, P.; Romeo, G. Study of conformational properties of poly(ethylene oxide) by SANS and PCS techniques. *Phys. Scr.* **2003**, *67*, 551−554.
(36) Matsudo, T.; Ogawa, K.; Kokufuta, E. Complex formation of protein with different water-soluble synthetic polymers. *Biomacromolecules* **2003**, *4*, 1794−1799.
(37) Drechsler, A.; Synytska, A.; Uhlmann, P.; Elmahdy, M. M.; Stamm, M.; Kremer, F. Interaction forces between microsized silica particles and weak polyelectrolyte brushes at varying pH and salt concentration. *Langmuir* **2010**, *26*, 6400−6410.
(38) Voronin, E. F.; Gun'ko, V. M.; Guzenko, N. V.; Pakhlov, E. M.; Nosach, L. V.; Leboda, R.; Skubiszewska-Zieba, J.; Malysheva, M. L.; Borysenko, M. V.; Chuiko, A. A. Interaction of poly(ethylene oxide) with fumed silica. *J. Colloid Interface Sci.* **2004**, *279*, 326−340.
(39) Gun'ko, V. M.; Voronin, E. F.; Zarko, V. I.; Goncharuk, E. V.; Turov, V. V.; Pakhovchishin, S. V.; Pakhlov, E. M.; Guzenko, N. V.; Leboda, R.; Skubiszewska-Zieba, J.; Janusz, W.; Chibowski, S.; Chibowski, E.; Chuiko, A. A. Interaction of poly(vinyl pyrrolidone) with fumed silica in dry and wet powders and aqueous suspensions. *Colloids Surf., A* **2004**, *233*, 63−78.
(40) Bekturov, E. A.; Bimendina, L. A. Interpolymer complexes. *Adv. Polym. Sci.* **1981**, *41*, 99−147.

(41) Khutoryanskiy, V. V.; Dubolazov, A. V.; Nurkeeva, Z. S.; Mun, G. A. pH effects in the complex formation and blending of poly(acrylic acid) with poly(ethylene oxide). *Langmuir* **2004**, *20*, 3785−3790.